BIOCHEMISTRY
including biophysical chemistry & molecular biology
Article

Biochemistry **2010,** *49,* 5533–5539 5533
DOI: 10.1021/bi100048y

Molecular Modeling Studies of Peptide Inhibitors Highlight the Importance of Conformational Prearrangement for Inhibition of Calpain†

Wanting Jiao, D. Quentin McDonald, James M. Coxon, and Emily J. Parker*

Department of Chemistry, University of Canterbury, Christchurch, New Zealand

Received January 12, 2010; Revised Manuscript Received May 14, 2010

ABSTRACT: The overexpression of the cysteine protease calpain is associated with many diseases, including brain trauma, spinal cord injury, Alzheimer's disease, Parkinson's disease, muscular dystrophy, arthritis, and cataract. Calpastatin is the naturally occurring specific regulator of calpain activity. It has previously been reported that a 20-mer peptide truncated from region B of calpastatin inhibitory domain 1 (named CP1B) retains both the affinity and selectivity of calpastatin toward calpain, exhibiting a K_i of 26 nM against μ-calpain, and is 1000-fold more selective for μ-calpain than cathepsin L. Both the wild-type and β-Ala mutant CP1B peptides exhibit a propensity to adopt a looplike conformation between Glu10 and Lys13. A computational study of human wild-type CP1B and the β-Ala mutants of this peptide was conducted. The resulting structural predictions were compared with the crystal structure of the calpain−calpastatin complex and were correlated with experimental IC_{50} values. These findings suggest that the conformational preference of the loop region between Glu10 and Lys13 of CP1B in the absence of calpain may contribute to the inhibitory activity of this series of peptides against calpain.

Calpain is a cysteine protease that is responsible for catalyzing the hydrolysis of the peptide bonds within a number of guest substrates. Substrates for calpain protease include calmodulin-binding proteins, the cytoskeletal proteins, and the G-proteins (*1*−*6*). The active site of calpain contains a highly conserved catalytic triad, which consists of Cys115, His272, and Asn296 (μ-calpain numbering). The sulfhydryl group of Cys115 acts as the nucleophile facilitating peptide bond cleavage.

Calpain requires the presence of calcium ions to be activated (*7*). The two major isoforms of calpain, μ- and m-calpain (also named calpain 1 and 2, respectively), are ubiquitous in nature and differ in their calcium requirements for activation. μ-Calpain requires a micromolar concentration of calcium ions, and m-calpain requires a millimolar calcium concentration to be activated in vitro. Overexpression of calpain is associated with many diseases, including brain trauma, spinal cord injury, Alzheimer's disease, Parkinson's disease, muscular dystrophy, arthritis, and cataract (*8*, *9*). In recent years, considerable effort has gone into developing small molecule inhibitors that are potent and selective for calpain as the pharmaceutical target (*8*).

The crystal structure of the inactive calcium-free human m-calpain has been reported (*10*). The protein consists of six domains (Figure 1), and these domains can be grouped into two subunits. The large subunit contains domains I−IV, and the small subunit contains domains V and VI. Domain II is the catalytic domain of calpain and contains the active site residues. This domain can be further subdivided into two subdomains, domain IIa and domain IIb, and both these subdomains contribute to the active site. Domain I is embedded in domain VI of the small subunit, helping hold the two subunits of the calpain molecule together in the inactive form. Domains IV and VI are the calcium binding domains. They each contain five EF-hands, which are typically helix−loop−helix substructures. Four of the five EF-hands can bind to calcium ions, and the fifth EF-hand in

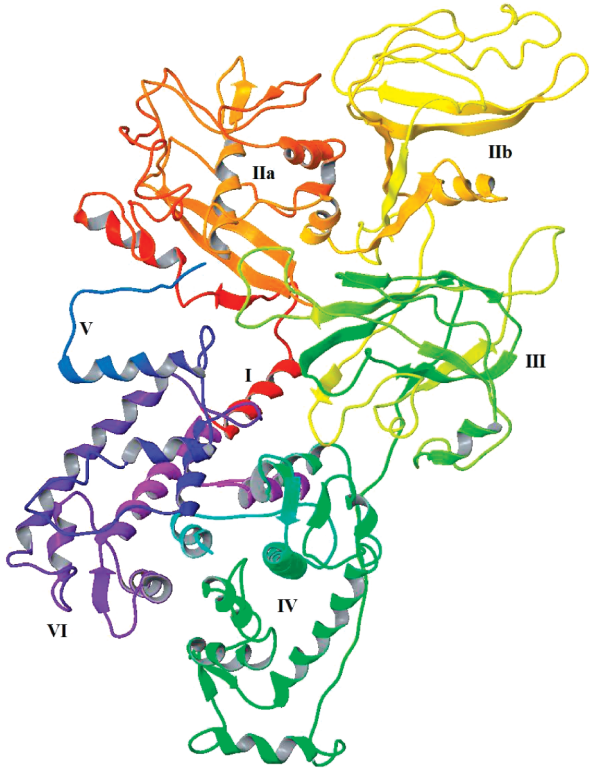

FIGURE 1: Crystal structure of calcium-free human m-calpain (Protein Data Bank entry 1KFU) (*10*).

†W.J. is a recipient of a New Zealand Tertiary Education Commission Top Doctoral Scholarship.

*To whom correspondence should be addressed: Department of Chemistry, University of Canterbury, Private Bag 4800, Christchurch, New Zealand. Telephone: (+64) 3 364 2871. Fax: (+64) 3 364 2110. E-mail: emily.parker@canterbury.ac.nz.

Published on Web 05/26/2010

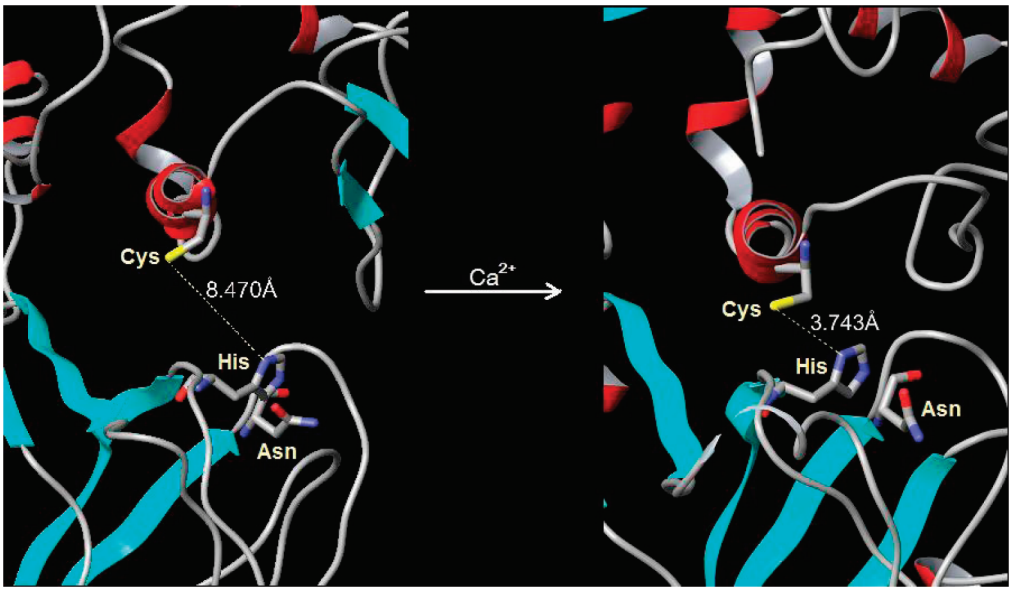

FIGURE 2: Catalytic triad in the human m-calpain active site before (Protein Data Bank entry IKFU) and after (Protein Data Bank entry 1MDW) activation by calcium (*10*, *39*).

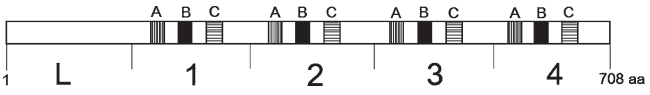

FIGURE 3: Schematic structure of human calpastatin.

each of domains IV and VI interacts with each other to form the heterodimer interface between the large and small subunits of calpain.

When calpain is in its inactive form, the two catalytic subdomains DIIa and DIIb are positioned apart from each other, and the distance between the active site cysteine and histidine is ~8 Å (Figure 2). Following activation by calcium ions, the separation between these two subdomains closes to complete the active site, and the distance between the active site cysteine and histidine reduces to 3−4 Å (Figure 2). This allows the histidine side chain to deprotonate the cysteine sulfhydryl group, assisting its nucleophilic role in the hydrolysis of an encapsulated peptide bond of the substrate.

Calpastatin coexists with calpain in the cell and is the naturally occurring calpain regulator, interacting specifically with calpain. Calpastatin is a unique peptide that has no known homologue (*11*). It is rich in polar and charged residues and has few hydrophobic residues.

Amino acid sequences of mammalian calpastatins have been determined by cDNA cloning. The deduced amino acid sequences of human, pig, rabbit, cow, and sheep calpastatins consist of 708, 713, 718, 705, and 723 residues, respectively (*12*−*16*). Human calpastatin has five domains (shown schematically in Figure 3). The L domain is at the N-terminus. Biological assays of the recombinant protein composed of domain L show that this domain does not inhibit either μ- or m-calpain (*17*−*19*). Domains 1−4 are four repetitive inhibitory domains, and each contains three highly conserved regions, A−C. The calpastatin molecule contains little secondary structure, with only regions A and C in each inhibitory domain having a tendency to form α-helical structures (*20*).

Each of the four repetitive inhibitory domains of calpastatin contains ~140 amino acid residues. These four domains have been individually expressed and assayed against calpain and have been shown to inhibit calpain independently (*21*−*23*). Regions A and C bind to domains IV and VI of calpain, respectively; region B binds in the active site to inhibit calpain (*24*, *25*).

A synthetic 27-mer peptide consisting of the central conserved sequence of region B of domain I of human calpastatin has been reported to possess potent inhibitory activity against pig μ- and m-calpain (*26*). This peptide is specific for calpain and exhibits no inhibitory activity against proteases papain or trypsin. In 1991, the solution structure of this 27-mer peptide was examined in DMSO-d_6 by two-dimensional ^{1}H NMR spectroscopy (*27*). There was no evidence found for any regular α-helix or β-sheet structure in this peptide, but there was a distinctive turn in the region from Glu10 to Lys13, which contains a highly conserved residue, Gly12. This suggests that although the repetitive domain of calpastatin does not have an extensive tertiary structure, it has a well-defined local turn structure in the well-conserved region that is proposed to be essential for the specific interaction with calpain. A combination of β-alanine scanning mutagenesis and kinetic measurements of the binding of the 27-mer peptide with calpain was used to probe the relative contributions of each amino acid to the overall calpain inhibitory activity (*28*). This study identified two important "hot spots", Leu11-Gly12 and Thr17-Ile18-Pro19, in the peptide that contain residues critical for inhibitory function. Mutation of any one of the key residues in either of the two regions resulted in a dramatic loss of inhibitory activity.

A 20-mer peptide with the amino acid sequence SSTYIEELGKREVTIPPKYR (sequence numbering starts at 4 and finishes at 23, to allow consistency with sequence numbering in the 27-mer peptide), identified by systematic truncation of the 27-mer peptide of calpastatin region B, has been reported to be the core sequence required to maintain affinity and selectivity toward calpain (*29*). This 20-mer peptide was named CP1B[1] to depict the region of calpastatin from which it was derived. The importance of the turnlike region between Glu10 and Lys13, which was identified earlier from the NMR studies of the 27-mer,

[1]Abbreviations: CP1B, 20-mer peptide resembling the core sequence of human calpastatin inhibitory domain 1 region B; WT, wild type; MCSD, stochastic dynamics (SD) combined with Monte Carlo sampling (MC); MD, molecular dynamics.

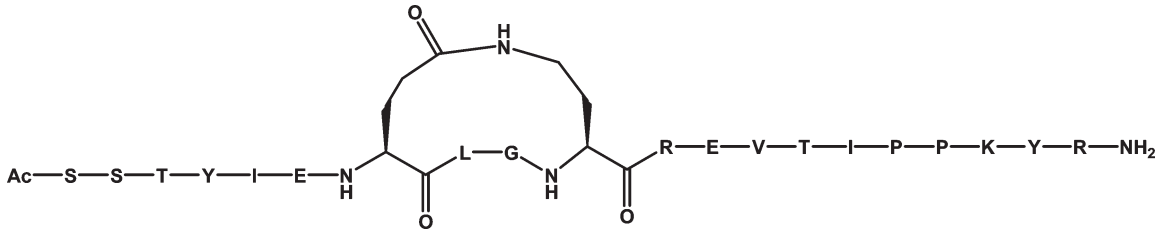

FIGURE 4: Structure of the macrocylic compound that is as potent as the linear CP1B peptide (*29*).

has been investigated by a study of a series of conformationally constrained macrocyclic variants of CP1B. These macrocyclic compounds were assayed against calpain, and the results showed one of these (Figure 4) was as potent as the "linear" CP1B peptide. Modeling showed that this macrocycle contained a looplike conformation in the region from amino acid 10 to 13. The high inhibitory activity of this macrocycle suggests that the activity of linear peptide CP1B is a consequence of it adopting a similar looplike conformation in the region between Glu10 and Lys13. This is further supported by the observation of a looplike conformation in this region in the crystal structure of the complex between calpastatin and m-calpain, which suggests the importance of this local structural feature of the calpastatin inhibitory domain B (*30*, *31*).

We report here a computational study of 20-mer peptide CP1B and various mutants in the absence of calpain. This study establishes the dynamic conformational preferences of these peptides, and the specific contribution of each residue near the Glu10−Lys13 region in dictating a looplike conformation. Using molecular dynamics analysis, these studies illuminate the importance of the prearrangement of this loop region in determining the inhibitory activity of CP1B.

MATERIALS AND METHODS

MCSD (*stochastic dynamics simulation combined with Monte Carlo sampling*). MCSD simulations for the CP1B wild type and selected β-Ala mutants were conducted with the modeling software package MacroModel using the OPLS2005 force field with the GB/SA water model to mimic the solvent effect (*32*).

For each mutant and the wild-type (WT) system of CP1B, three repetitive (50 ns each) simulations were conducted starting with similar linear conformations. The starting linear conformation of the WT peptide CP1B was established using the protein builder in Schrodinger GUI Maestro (*33*). The analogous starting conformations for the various mutants of CP1B were generated by mutating corresponding residues of WT CP1B into β-Ala in silico, in line with the experimental changes made to the peptide by Betts et al. (*28*).

For WT CP1B, two other MCSD simulations (50 ns each) were conducted starting with half-folded and fully folded conformations. The half-folded starting conformation of WT CP1B was the conformation in the last frame of a 1 ns molecular dynamics simulation for CP1B. The starting fully folded conformation used in these calculations was the lowest-energy conformer obtained from a conformational search for the WT peptide. This conformational search was conducted with the MCMM Serial Torsional Sampling method and was run with a GB/SA water model, using the OPLS2005 force field, with 3000 steps for the conformational search and an energy window of 12.0 kJ/mol for collecting appropriate conformers.

For all MCSD simulations conducted in this study, there was no cutoff distance applied for electronic and van der Waals interactions. The starting structure in each case was first minimized for up to 5000 steps with a gradient convergence threshold of 0.05. Stochastic dynamics was then conducted for 50 ns with the SHAKE procedure applied to all bonds to hydrogen atoms. The simulations were run at a constant temperature of 300 K and with a time step of 1.5 fs (*34*). During the dynamics simulation, the torsions within the peptide were subject to changes by the application of the Monte Carlo method. Five hundred structures were sampled in equal time intervals for later examination and analysis.

Molecular Dynamics with NAMD. To confirm that the conformations obtained from MCSD simulations were reasonable, three 100 ns long molecular dynamics (MD) simulations for WT CP1B were conducted with NAMD running on the BlueFern supercomputer at the University of Canterbury (*35*). The starting conformations of these three MD simulations were obtained from the final frames in the three MCSD simulations for WT CP1B starting from linear, half-folded, and folded conformations as described above. The peptides were solvated with explicit water molecules in a water box. The water box in each system contains approximately 1500−1600 water molecules. The simulations were conducted with CHARMM force field parameter specifications at a constant temperature of 300 K and a constant pressure of 1 atm (*36*). The cutoff distance for van der Waals interactions was set to 12 Å. In each simulation, the system was first minimized for 5000 steps followed by 100 ns of dynamics simulation conducted with 2 fs time steps. The trajectory was written out at the 100 ps time interval, and a total of 1000 frames were obtained from each simulation (100 ns). These full-atom MD simulations are significantly more computationally expensive than the MCSD method. With NAMD using 32 processors running on the BlueFern supercomputer, each of the three 100 ns MD simulations takes 3−5 weeks to complete.

The results of these MD simulations with WT CP1B were compared with the MCSD simulation to establish the validity of using the less expensive MCSD method. This is discussed below.

Cluster Analysis of Sampled Conformations. Cluster analyses were conducted on the sampled structures using XCluster (*37*) to examine the conformations explored during the MCSD and MD simulations. The clustering was performed in a hierarchical fashion, based on the pairwise root-mean-square displacements (rmsd) of selected comparison atoms. In this study, the comparison atoms were set to be the backbone heavy atom of the loop region of Glu10−Lys13 for the WT CP1B system and the region of Glu9−Glu15 for the β-Ala mutant systems. The clusters with the most members were considered to comprise the most stable conformations explored during the dynamics simulations, and the representative structures of the largest clusters found in these simulations were selected as follows. For each cluster, the centroid of each of the comparison

Table 1: Cluster Analyses of Sampled Structures from the MCSD and MD Simulations for WT CP1B

simulation	simulation duration (ns)	simulation type	no. of clusters	cluster size
1	50	MCSD	2	270, 230
2	50	MCSD	3	152, 1, 347
3	50	MCSD	2	499, 1
4	100	MD	3	35, 64, 1
5	100	MD	4	9, 8, 8, 75
6	100	MD	4	90, 1, 8, 1

Table 2: Overall and Loop Region Backbone rmsd Values in the Three 50 ns MCSD Simulations for the WT CP1B Peptide[a]

simulation	simulation duration (ns)	starting conformation	backbone rmsd (Å)	loop region (Glu10−Lys13) backbone rmsd (Å)
1	50	linear	16.8	2.22
2	50	half-folded	10.7	1.97
3	50	folded	2.23	0.30

[a]The rmsd values are measured between the starting conformation and the representative structure of the largest cluster in each simulation.

atoms was determined. Then the structure within the cluster which had the minimum rms interatomic distance from these centroids was selected as the most representative structure of this cluster. These representative structures were then used in further structural comparisons.

RESULTS AND DISCUSSION

Dynamics of WT CP1B. To examine the conformational preference of the WT CP1B peptide, particularly the proposed loop region (from Glu10 to Lys13), in the absence of the calpain enzyme, stochastic dynamics simulations incorporating Monte Carlo sampling (MCSD) were conducted for the WT system.

Three MCSD (50 ns) simulations of the WT CP1B peptide were initiated starting from linear, half-folded, and fully folded conformations. Cluster analyses aimed to examine the conformations explored during these simulations were conducted (Table 1). In the cluster analyses, pairwise rms displacements in backbone atoms of the loop region (Glu10−Lys13) were calculated, and the sampled structures were clustered on the basis of these displacements. The largest cluster in each simulation was considered to comprise the most stable conformations explored, and the representative structure of all members in the largest cluster was obtained to be used in further structural comparisons. The backbone rmsd values for the entire peptide and the loop region (Glu10−Lys13) between the representative structures and the starting conformations in these simulations are listed in Table 2. rmsd measurements for two of the MCSD simulations [simulations 1 and 2 (Table 2)], starting from the linear and half-folded conformations, were large, indicating the MCSD method is sampling significant conformational space. Simulation 3 which started with the folded conformation shows much smaller backbone changes. This is consistent with the folded starting conformation for this calculation representing a low-energy conformer of the WT CP1B peptide. Therefore, this simulation started from a favorable low-energy conformation and exhibited limited sampling outside this local minimum during the entire simulation.

To ensure efficient sampling over large conformational space, all further MCSD simulations for both WT CP1B and its mutants were set to begin with the extended linear conformations. The backbone rmsd values for the loop region (Table 2) were generally found to be smaller than the overall backbone rmsd variation but still gave the same trend, with simulations 1 and 2 producing larger rmsd values than simulation 3. Importantly, all three simulations resulted in folded conformations (see Table S1 of the Supporting Information), demonstrating that the peptide has a strong preference for an overall folded looplike conformation.

The MCSD method treats solvent implicitly and combines stochastic dynamics with Monte Carlo sampling. To exclude the possibility that folding observed in simulations 1 and 2 was an artifact of this particular simulation method, the conformations obtained from the last frames in these three MCSD simulations were used as the starting geometries for three more rigorous 100 ns MD simulations, in which the solvent was treated explicitly. This was done to establish if the loop region between Glu10 and Lys13 would start to unfold.

Examination of the simulation ensembles showed that the loop region (Glu10−Lys13) of WT CP1B remained folded during these three 100 ns MD simulations (see Table S2 of the Supporting Information). The conformation of the loop region was generally observed to become stable more than 35 ns into the MD simulation (see Figure S3 of the Supporting Information). The same cluster analyses as described above were conducted to examine the sampled structures from these three MD simulations (Table 1), and the representative structures of the largest clusters were obtained for structural comparison (see Table S2 of the Supporting Information for superposition of the representative structures and the starting conformations). The rmsd values of the loop region backbone were reasonably small (within 0.8 Å for simulations 4 and 6 and slightly larger in simulation 5, with a rmsd value of 1.84 Å) considering the system under study was a small flexible peptide (Table 3). This suggests that both the full-atom MD and the MCSD simulations are sampling in the same family of related loop conformations for the Glu10−Lys13 region. This validates the use of the less computationally expensive MCSD method for the following study and furthermore confirms that the peptide indeed has an inherent propensity to fold.

The modeling results obtained for WT CP1B can be compared with two crystal structures of the calpain−calpastatin complex recently reported by Moldoveanu et al. (*31*) and Hanna et al. (*30*), which illustrate the interactions between region B of calpastatin and the active site of calpain at the atomic level. In these two crystal structures, the section of region B of calpastatin that corresponds to 20-mer peptide CP1B was found to bind within the active site cleft of calpain (Figure 5).

The binding conformation of the loop region of CP1B in the crystal structure (Protein Data Bank entry 3DF0) was used as the reference structure, and the backbone rmsd values for the loop region (Glu10−Lys13) were measured for all representative structures in the three MCSD simulations for WT CP1B (Table 4) (see Table S1 of the Supporting Information for superposition of the representative structures and the binding conformation). All three simulations showed reasonably small backbone rmsd values for the loop region, with simulation 1 displaying the smallest rmsd value (0.75 Å). The comparison between the crystal structure conformation and our modeling results suggests that even in the absence of the calpain enzyme,

Table 3: Backbone rmsd Values of the Loop Region in the Three 100 ns MD Simulations[a]

simulation	simulation duration (ns)	starting conformation	loop region (Glu10−Lys13) backbone rmsd (Å)
4	100	last frame structure of simulation 1	0.73
5	100	last frame structure of simulation 2	1.84
6	100	last frame structure of simulation 3	0.74

[a]The rmsd values are measured between the starting conformation and the representative structure of the largest cluster in each simulation.

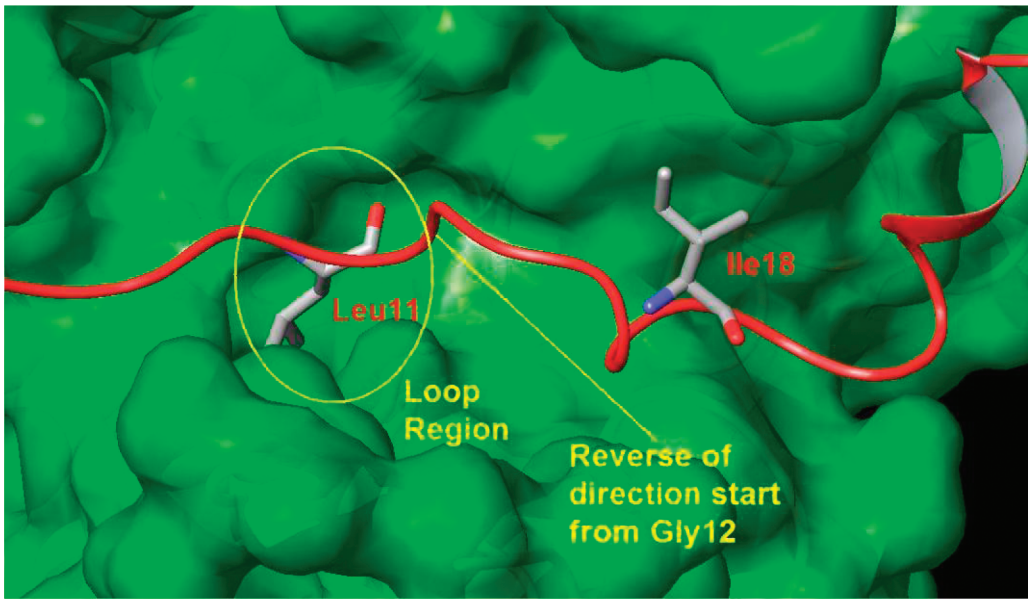

FIGURE 5: Active site of calpain bound with a calpastatin molecule in the crystal structure of Protein Data Bank entry 3DF0, where calpastatin is colored red. The key residues Leu11 and Ile18 in region B of calpastatin are displayed as tubes. The proposed looplike region is highlighted in the yellow circle.

Table 4: Backbone rmsd Values of the Loop Region (Glu10−Lys13) between the Binding Conformation of CP1B in Crystal Structure 3DF0 and the Representative Structures in the Largest Clusters of Each MCSD Simulation for WT CP1B

simulation	starting conformation	loop region (Glu10−Lys13) backbone rmsd compared to the binding conformation (Å)
1	linear	0.75
2	half-folded	1.17
3	folded	0.79

the region of Glu10−Lys13 of WT CP1B has a propensity to fold into looplike conformations that are very similar to the conformation known to bind.

Dynamics of Selected β-Ala Mutants of CP1B and Conformational Analysis. Following the studies of WT CP1B, studies were undertaken to establish the effect of mutations along the peptide on the conformational preference of this loop region in the absence of calpain. A prior study reported experimental IC_{50} values of various β-Ala mutants of the CP1B peptide (*28*). Therefore, we elected to carry out β-Ala mutations in silico along the CP1B peptide to provide direct comparison with the reported experimental IC_{50} values.

A series of β-Ala mutants of CP1B were obtained by selective mutation of residues Glu9, Glu10, Gly12, Lys13, Arg14, and Glu15, near the proposed loop region in silico. Residue Leu11 was omitted from this study because it has been shown that the importance of this residue in calpain inhibition lies in its side chain functionality (*38*). The side chain of Leu11 acts to fit in one hydrophobic pocket in the calpain active site, and losing this interaction (by β-Ala mutation) dramatically decreases the level of inhibition of calpain by the CP1B peptide. Therefore, the effect of the Leu11βAla mutation on the measured IC_{50} value is mainly contributed by the loss of its side chain functionality, rather than its possible effect on the conformation of this loop region. Unlike Leu11, the other residues (Glu9, Glu10, and Gly12−Glu15) are likely to play a role in facilitating the formation of the looplike conformation (*29*). The oppositely charged residues on either side of the loop region (Glu9, Glu10, Lys13, and Arg14) can form salt bridges that would bring the two ends of the loop region into the proximity of each other, and the highly flexible Gly12 can act to promote the formation of the loop.

For each β-Ala mutant, three repetitive MCSD simulations (50 ns) were initiated from similar linear conformations to enhance the likelihood that the conformational space is appropriately traversed. All MCSD simulations for all six β-Ala mutants produced folded looplike conformations. A cluster analysis was conducted for each simulation to examine the conformations explored (Table 5). In these cluster analyses, the pairwise backbone displacements in the region from Glu9 to Glu15 were calculated between all sampled structures in each simulation. The largest cluster was identified for each simulation, and the representative structure was obtained to be used in the following structural comparisons. An rmsd analysis was then

Table 5: Cluster Analyses of Sampled Structures from MCSD Simulations for Various β-Ala Mutants of CP1B

species	simulation	no. of clusters	cluster sizes
Glu9bβAla	Glu9βAla_1	2	1, 499
	Glu9βAla_2	2	499, 1
	Glu9βAla_3	3	1, 3, 496
Glu10βAla	Glu10βAla_1	5	2, 1, 72, 1, 424
	Glu10βAla_2	2	499, 1
	Glu10βAla_3	2	8, 492
Gly12βAla	Gly12βAla_1	2	1, 499
	Gly12βAla_2	2	498, 2
	Gly12βAla_3	4	496, 2, 1, 1
Lys13βAla	Lys13βAla_1	3	14, 485, 1
	Lys13βAla_2	4	495, 2, 2, 1
	Lys13βAla_3	3	496, 2, 2
Arg14βAla	Arg14βAla_1	2	499, 1
	Arg14βAla_2	4	1, 1, 9, 489
	Arg14βAla_3	2	1, 499
Glu15βAla	Glu15βAla_1	3	2, 22, 476
	Glu15βAla_2	4	34, 464, 1, 1
	Glu15βAla_3	2	499, 1

used to examine the effect of these β-Ala mutations on the conformational preference of the loop region of CP1B. To ensure that the effect of any particular mutation was not over-represented, rmsd values are measured for the region from Glu9 to Glu15; i.e., all the mutated residues are included in rmsd calculations. Backbone heavy atom rmsd values for the region of Glu9−Glu15 were measured between the binding conformation of CP1B in the crystal structure (Protein Data Bank entry 3DF0) and the representative structures obtained from cluster analysis for the simulation ensembles of β-Ala mutants of CP1B (Table 6) (see Table S4 of the Supporting Information for superposition of representative structures and the binding conformation). The rmsd values provide measures of deviation from the binding conformation in the loop region for each of the six β-Ala mutants. These in turn can give an indication of the effect of different β-Ala mutations on the conformations and possible prearrangement of the loop region.

The variations in rmsd values (Table 6) for the different mutant systems demonstrated that the mutations have indeed altered the conformations of the loop region. The largest rmsd deviations were found for the Gly12βAla mutant system, indicating that the Gly12βAla mutation has the greatest effect on the conformation of the loop region. This in turn suggests that Gly12 is important for adoption of a looplike conformation in the region of Glu10−Lys13 prior to interaction with calpain. In contrast, Glu9βAla, Glu15βAla, and Lys13βAla systems exhibited relatively smaller deviations from the bound conformation, suggesting that these residues have a smaller influence on the loop conformation.

To establish if there is a trend in the effect of the mutations on the conformational preference of the loop region, the average rmsd values for each mutant system were compared (Table 6). The deviations from the binding conformation in the mutant systems are thereby ranked in the following order: Glu15 < Arg14 < Lys13 < Glu9 < Glu10 < Gly12. The larger deviation of the loop region from the binding conformation indicates the stronger influence of the corresponding mutation on the conformation of the loop region and, in turn, indicates the greater contribution that the mutated residue makes to the conformational preference of the loop region. The rank of individual residue contribution to the conformational preference of the loop region or loop prearrangement in the absence of calpain (termed the "conformational rank") will be in the same order as above.

Table 6: Backbone rmsd Values for the Region of Glu9−Glu15 between the Binding Conformation of CP1B in the Crystal Structure (3DF0) and the Representative Structure Obtained from Each MCSD Simulation for the β-Ala Mutants of CP1B[a]

species	simulation	backbone rmsd between the representative structure and the binding conformation (Å)	average rmsd (Å)
Glu9βAla	Glu9βAla_1	2.80	3.58
	Glu9βAla_2	3.82	
	Glu9βAla_3	4.12	
Glu10βAla	Glu10βAla_1	4.76	4.88
	Glu10βAla_2	5.26	
	Glu10βAla_3	4.63	
Gly12βAla	Gly12βAla_1	5.68	5.43
	Gly12βAla_2	5.83	
	Gly12βAla_3	4.78	
Lys13βAla	Lys13βAla_1	3.09	3.36
	Lys13βAla_2	3.43	
	Lys13βAla_3	3.57	
Arg14βAla	Arg14βAla_1	4.08	3.13
	Arg14βAla_2	3.42	
	Arg14βAla_3	1.89	
Glu15βAla	Glu15βAla_1	3.29	3.10
	Glu15βAla_2	2.17	
	Glu15βAla_3	3.85	

[a]The average rmsd is the average rmsd value in the three repetitive MCSD simulations for each mutant system.

Previously, Betts et al. have reported a rank of individual residue contribution to inhibitory activity based on the experimentally measured IC_{50} values for a series β-Ala mutants (*28*). In this "functional rank", the contributions of the mutated residues near the loop region to the inhibition activity were placed in the following order: Glu15 < Lys13 < Glu9 < Glu10 < Arg14 < Gly12.

The conformational rank was based on only the conformational preferences of the CP1B mutants in the absence of calpain, while the functional rank takes into account not only the conformational factors but also other contributing factors such as the interactions between the peptide variants and calpain active site. However, comparison between the conformational rank from our modeling study and the functional rank from experimental measurements shows that the two ranks are remarkably closely correlated, with the only exception being Arg14. This difference in ranking for Arg14 may suggest that the effect of Arg14 on calpain inhibition is mainly contributed by the side chain functionality and the interactions with the calpain active site, rather than its effect on the preference of the loop region conformation. However, the striking similarity of the general trend in the ranking obtained from both experimental and computational methods suggests that the differences in the conformational preferences of the loop region in CP1B mutants may be a significant contributing factor to their ability to inhibit calpain.

In summary, MD calculations have been used to demonstrate that a series of calpain inhibitors derived from natural regulator calpastatin have a preference for a adopting the looplike conformation that is associated with binding in the absence of calpain. The inhibitory activity of these peptides can be correlated to the propensity of these peptides to prearrange in a looplike

conformation. Therefore, the ability to preadopt looplike conformations is an important factor for the design of effective inhibitors of calpain.

SUPPORTING INFORMATION AVAILABLE

Tables of simulation ensembles of the MCSD and MD simulations for WT CP1B and mutants and rmsd plots of the three 100 ns MD simulations. This material is available free of charge via the Internet at http://pubs.acs.org.

REFERENCES

1. Wang, K. K., Villalobo, A., and Roufogalis, B. D. (1989) Calmodulin-binding proteins as calpain substrates. *Biochem. J. 262*, 693–706.
2. Croall, D. E., and Demartino, G. N. (1991) Calcium-activated neutral protease (calpain) system: Structure, function, and regulation. *Physiol. Rev. 71*, 813–847.
3. Greenwood, A. F., and Jope, R. S. (1994) Brain G-protein proteolysis by calpain: Enhancement by lithium. *Brain Res. 636*, 320–326.
4. Bi, X. N., Tocco, G., and Baudry, M. (1994) Calpain-mediated regulation of ampa receptors in adult rat brain. *NeuroReport 6*, 61–64.
5. Hirai, S., Kawasaki, H., Yaniv, M., and Suzuki, K. (1991) Degradation of transcription factors, C-jun and C-fos, by calpain. *FEBS Lett. 287*, 57–61.
6. Watt, F., and Molloy, P. L. (1993) Specific cleavage of transcription factors by the thiol protease, m-calpain. *Nucleic Acids Res. 21*, 5092–5100.
7. Goll, D. E., Thompson, V. F., Li, H., Wei, W. E. I., and Cong, J. (2003) The calpain system. *Physiol. Rev. 83*, 731–801.
8. Donkor, I. O. (2000) A survey of calpain inhibitors. *Curr. Med. Chem. 7*, 1171–1188.
9. Zatz, M., and Starling, A. (2005) Calpains and disease. *N. Engl. J. Med. 352*, 2413–2423.
10. Strobl, S., Fernandez-Catalan, C., Braun, M., Huber, R., Masumoto, H., Nakagawa, K., Irie, A., Sorimachi, H., Bourenkow, G., Bartunik, H., Suzuki, K., and Bode, W. (2000) The crystal structure of calcium-free human m-calpain suggests an electrostatic switch mechanism for activation by calcium. *Proc. Natl. Acad. Sci. U.S.A. 97*, 588–592.
11. Takano, E., and Maki, M. (1999) Structure of calpastatin and its inhibitory control of calpain. In Calpain: Pharmacology and Toxicology of Calcium-Dependent Protease (Wang, K. K. W., and Yuen, P.-w., Eds.) pp 25−50, Taylor & Francis, New York.
12. Asada, K., Ishino, Y., Shimada, M., Shimojo, T., Endo, M., Kimizuka, F., Kato, I., Maki, M., Hatanaka, M., and Murachi, T. (1989) cDNA cloning of human calpastatin: Sequence homology among human, pig, and rabbit calpastatins. *J. Enzyme Inhib. 3*, 49–56.
13. Lee, W. J., Ma, H., Takano, E., Yang, H. Q., Hatanaka, M., and Maki, M. (1992) Molecular diversity in amino-terminal domains of human calpastatin by exon skipping. *J. Biol. Chem. 267*, 8437–8442.
14. Takano, E., Maki, M., Mori, H., Hatanaka, M., Marti, T., Titani, K., Kannagi, R., Ooi, T., and Murachi, T. (1988) Pig-heart calpastatin: Identification of repetitive domain-structures and anomalous behaviour in polyacrylamide gel electrophoresis. *Biochemistry 27*, 1964–1972.
15. Emori, Y., Kawasaki, H., Imajoh, S., Imahori, K., and Suzuki, K. (1987) Endogenous inhibitor for calcium-dependent cysteine protease contains 4 internal repeats that could be responsible for its multiple reactive sites. *Proc. Natl. Acad. Sci. U.S.A. 84*, 3590–3594.
16. Killefer, J., and Koohmaraie, M. (1994) Bovine skeletal-muscle calpastatin: Cloning, sequence-analysis, and steady-state messenger-RNA expression. *J. Anim. Sci. 72*, 606–614.
17. Melloni, E., Tullio, R. D., Averna, M., Tedesco, I., Salamino, F., Sparatore, B., and Pontremoli, S. (1998) Properties of calpastatin forms in rat brain. *FEBS Lett. 431*, 55–58.
18. Averna, M., De Tullio, R., Salamino, F., Melloni, E., and Pontremoli, S. (1999) Phosphorylation of rat brain calpastatins by protein kinase C. *FEBS Lett. 450*, 13–16.
19. Melloni, E., Averna, M., Stifanese, R., De Tullio, R., Defranchi, E., Salamino, F., and Pontremoli, S. (2006) Association of calpastatin with inactive calpain: A novel mechanism to control the activation of the protease? *J. Biol. Chem. 281*, 24945–24954.
20. Kiss, R., Kovacs, D., Tompa, P., and Perczel, A. (2008) Local structural preferences of calpastatin, the intrinsically unstructured protein inhibitor of calpain. *Biochemistry 47*, 6936–6945.
21. Maki, M., Takano, E., Mori, H., Sato, A., Murachi, T., and Hatanaka, M. (1987) All four internally repetitive domains of pig calpastatin possess inhibitory activities against calpains I and II. *FEBS Lett. 223*, 174–180.
22. Emori, Y., Kawasaki, H., Imajoh, S., Minami, Y., and Suzuki, K. (1988) All four repeating domains of the endogenous inhibitor for calcium-dependent protease independently retain inhibitory activity. Expression of the cDNA fragments in *Escherichia coli*. *J. Biol. Chem. 263*, 2364–2370.
23. Hanna, R. A., Garcia-Diaz, B. E., and Davies, P. L. (2007) Calpastatin simultaneously binds four calpains with different kinetic constants. *FEBS Lett. 581*, 2894–2898.
24. Todd, B., Moore, D., Deivanayagam, C. C. S., Lin, G. D., Chattopadhyay, D., Maki, M., Wang, K. K. W., and Narayana, S. V. L. (2003) A structural model for the inhibition of calpain by calpastatin: Crystal structures of the native domain VI of calpain and its complexes with calpastatin peptide and a small molecule inhibitor. *J. Mol. Biol. 328*, 131–146.
25. Nishimura, T., and Goll, D. E. (1991) Binding of calpain fragments to calpastatin. *J. Biol. Chem. 266*, 11842–11850.
26. Maki, M., Takano, E., Osawa, T., Ooi, T., Murachi, T., and Hatanaka, M. (1988) Analysis of structure-function relationship of pig calpastatin by expression of mutated cDNAs in *Escherichia coli*. *J. Biol. Chem. 263*, 10254–10261.
27. Ishima, R., Tamura, A., Akasaka, K., Hamaguchi, K., Makino, K., Murachi, T., Hatanaka, M., and Maki, M. (1991) Structure of the active 27-residue fragment of human calpastatin. *FEBS Lett. 294*, 64–66.
28. Betts, R., Weinsheimer, S., Blouse, G. E., and Anagli, J. (2003) Structural determinants of the calpain inhibitory activity of calpastatin peptide B27-WT. *J. Biol. Chem. 278*, 7800–7809.
29. Pfizer, J., Assfalg-Machleidt, I., Machleidt, W., and Schaschke, N. (2008) Inhibition of human μ-calpain by conformationally constrained calpastatin peptides. *Biol. Chem. 389*, 83–90.
30. Hanna, R. A., Campbell, R. L., and Davies, P. L. (2008) Calcium-bound structure of calpain and its mechanism of inhibition by calpastatin. *Nat. Lett. 456*, 409–412.
31. Moldoveanu, T., Gehring, K., and Green, D. R. (2008) Concerted multi-pronged attack by calpastatin to occlude the catalytic cleft of heterodimeric calpains. *Nat. Lett. 456*, 404–408.
32. MacroModel, version 9.1 (2005) Schrödinger, LLC, New York.
33. Maestro, version 7.5 (2005) Schrodinger, LLC, New York.
34. Ryckaert, J.-P., Ciccotti, G., and Berendsen, H. J. C. (1977) Numerical integration of the Cartesian equation of motion of a system with constraints: Molecular dynamics of N-alkanes. *J. Comput. Phys. 23*, 327.
35. Phillips, J. C., Braun, R., Wang, W., Gumbart, J., Tajkhorshid, E., Villa, E., Chipot, C., Skeel, R. D., Kale, L., and Schulten, K. (2005) Scalable molecular dynamics with NAMD. *J. Comput. Chem. 26*, 1781–1802.
36. MacKerell, A. D., Jr., Bashford, D., Bellott, M., Dunbrack, R. L., Jr., Evanseck, J. D., Field, M. J., Fischer, S., Gao, J., Guo, H., Ha, S., Joseph-McCarthy, D., Kuchnir, L., Kuczera, K., Lau, F. T. K., Mattos, C., Michnick, S., Ngo, T., Nguyen, D. T., Prodhom, B., Reiher, W. E., III, Roux, B., Schlenkrich, M., Smith, J. C., Stote, R., Straub, J., Watanabe, M., Wiórkiewicz-Kuczera, J., Yin, D., and Karplus, M. (1998) All-atom empirical potential for molecular modeling and dynamics studies of proteins. *J. Phys. Chem. B 102*, 3586–3616.
37. Shenkin, P. S., and McDonald, D. Q. (1994) Cluster Analysis of Molecular Conformations. *J. Comput. Chem. 15*, 899–916.
38. Betts, R., and Anagli, J. (2004) The β- and γ-CH2 of B27-WT's Leu11 and Ile18 side chains play a direct role in calpain inhibition. *Biochemistry 43*, 2596–2604.
39. Moldoveanu, T., Hosfield, C. M., Lim, D., Jia, Z. C., and Davies, P. L. (2003) Calpain silencing by a reversible intrinsic mechanism. *Nat. Struct. Biol. 10*, 371–378.